To be submitted to
Riv. Nuovo Cimento

ISTITUTO NAZIONALE DI FISICA NUCLEARE
Laboratori Nazionali di Frascati

LNF-80/45(P)
30 Luglio 1981
(Revised Version 15 Luglio 1981

M. Piacentini:

MODULATION SPECTROSCOPY WITH SYNCHROTRON RADIATION.

Servizio Documentazione
dei Laboratori Nazionali di Frascati
Cas. Postale 13 - Frascati (Roma)

INFN - Laboratori Nazionali di Frascati
Servizio Documentazione

LNF-80/45(P)
30 Luglio 1980
(Revised Version 15 Luglio 1981)

M. Piacentini[(*)]: MODULATION SPECTROSCOPY WITH SYNCHROTRON RADIATION.

ABSTRACT

Modulation spectroscopy performed using synchrotron radiation as a light source in the vacuum ultraviolet and soft x-rays regions has been reviewed critically. Particular emphasis was given to the experiments performed on insulators and metals, since semiconductors have been dealt with in detail by other authors. For each experiment or group of experiments, we tried to give a picture of the status of the research before the experiment was perfomed, and then to describe the new results. In some cases they could enlighten some controversies, in other cases they opened new questions and new fields of research.

1. - INTRODUCTION

The study of the optical properties of solids in the far ultraviolet and soft x-ray regions received a strong push by the spread and development of synchrotron radiation facilities. The continuous and intense nature of synchrotron radiation allowed studying with great accuracy a large variety of materials and the discovery of the main phenomena associated with photoabsorption[(1)]. In the lowest energy region, up to about 20-25 eV, the excitation of the valence electrons still gives strong structures, while at higher energies the core electrons also are excited. The absorption spectra of the core electrons extend several tens or hundreds of eV beyond threshold with significant, but broad, structures, mostly originating from atomic effects. Instead, rather sharp features appear within the first 10-15 eV beyond the threshold, features associated with solid state excitations: interband transitions with critical point and density of states structures, excitons, many-body effects. But even if "sharp", these features are rather broad,

(*) Gruppo PULS, Laboratori Nazionali dell'INFN, Frascati - Italy and Gruppo Nazionale di Struttura delle Materia del CNR, Roma.

typically 0.5-1.0 eV wide, in comparison with the valence band features (usually of the order of 0.01 eV). Thus, in many cases a detailed and unambiguous interpretation of the spectra could not be carried out in spite of the large wealth of data accumulated.

In the quartz optic region (from infrared to ultraviolet), modulation spectroscopy has proven to be of invaluable help for refining and improving our understanding of the electronic processes underlying the optical spectra[2,3]. The reason stems from the simple fact that, by applying a small periodic perturbation to a sample (for example, an electric field) and by measuring directly the induced change of its optical properties, one is capable of enhancing weak structures, of resolving closely spaced transitions, and of being sensitive only to some types of transitions that often are blurred in the strong background of all other types of degenerate transitions. In addition, the proper choice of the external perturbing field is important for extracting certain characteristics of the transitions.

The extension of modulation spectroscopy to the far ultraviolet was then looked forward to by scientists, even if some skepticism about such a possibility was widespread. In fact, the feeling was that the broadening due to the shorter lifetimes of the excited states would tend to wash out any structure and make modulation spectroscopy unimportant at higher energies. Only with the recent advent of storage rings as stable sources[4], modulation spectroscopy was attempted in the far ultraviolet, above 10 eV. The first results were striking and promising. In fact, the thermoreflectance spectrum of gold, measured by Piacentini et al.[5,6] showed several sharp structures, up to about 35 eV. The width of these structures was limited by the monochromator resolution of 0.1 eV. In the same region the reflectivity of gold is rather smooth, the only significant feature being a 6 eV wide peak at 22 eV.

The full potentiality of modulation spectroscopy was thus extended also to the synchrotron radiation spectral range. Since then, it has become a routine technique and already it has given a great deal of new information on the photoabsorption processes in several classes of materials. In some cases it helped to discriminate between different interpretations given to the same spectral feature; in other cases it opened new questions.

Modulation spectroscopy with synchrotron radiation has been reviewed recently by Aspnes[7], who stressed the applications to semiconductors. Lynch[8,9] reported the results obtained with the modulation technique as a contribution to the more general field of synchrotron radiation spectroscopy. In this paper we shall review the main results obtained by modulation spectroscopy expecially on insulators and metals. We shall try to give a picture of the general understanding of the electronic properties of the investigated materials when the modulation experiment was performed, and then we shall discuss the new contributions and the studies that have been stimulated. This review will deal only with proper modulation experiments, i.e. with those in which one of the parameters defining the state of the sample, such as the temperature or an external field, is periodically changed. "Differential" spectra are available from the literature too, spectra that have been obtained by subtracting from each other the spectra measured on samples under different conditions, for example, at different temperatures[10]. In these very last years another form of "differential" spectra have been reported: they are first and second-energy (or wavelength) derivatives calculated numerically from very precise transmission or reflectivity spectra[11]. Since both types of spectra are derived off-line from the experiment and serve only to enhance weak structures already present in the direct measurements, they will be not considered in this review.

2. - EXPERIMENTAL

Modulation spectroscopy is a well known technique[2,3] and we shall not enter into the details here, except for those developments required for working in the far ultraviolet. Let us recall briefly some considerations on the optical constants of solids[12,13], with the main purpose of introducing the nomenclature to be used later on.

The response of a medium to an external electromagnetic wave of angular frequency ω can be described by its complex dielectric function $\tilde{\varepsilon}(\omega) = \varepsilon_1(\omega) + i\,\varepsilon_2(\omega)$. The knowledge of $\tilde{\varepsilon}(\omega)$ allows one to obtain all the other optical constants of the medium according to Table I.

TABLE I

Optical constants of an isotropic medium and their relations. ω and λ correspond to the angular frequency and the wavelength of the radiation respectively; $\underline{q}$ is the excitation transferred momentum; ϑ is the angle of incidence of the radiation, that can be linearly polarized either parallel (s) or perpendicular (p) to the plane of incidence; d is the thickness of the sample.

Dielectric function(x)	$\tilde{\varepsilon}(\omega,\underline{q}) = \varepsilon_1(\omega,\underline{q}) + i\varepsilon_2(\omega,\underline{q})$	
Refractive index(x)	$\tilde{N}(\omega) = n(\omega) + ik(\omega)$	$= \sqrt{\tilde{\varepsilon}(\omega)}$
Conductivity(x)	$\tilde{\sigma}(\omega) = \sigma_1(\omega) + i\sigma_2(\omega)$	$= \frac{\omega}{4\pi} i\tilde{\varepsilon}$
Loss function(x)(o)	$\tilde{\mathcal{L}}(\omega,\underline{q}) = \mathcal{L}_1(\omega,\underline{q}) + i\mathcal{L}_2(\omega,\underline{q})$	$= \tilde{\varepsilon}(\omega,\underline{q})^{-1}$
Fresnel coefficients(x)	$\tilde{r}_s(\omega,\vartheta) = \sqrt{R_s(\omega,\vartheta)}\, e^{i\varphi_s(\omega,\vartheta)}$	$= \frac{\cos\vartheta - \sqrt{\tilde{\varepsilon}(\omega) - \sin^2\vartheta}}{\cos\vartheta + \sqrt{\tilde{\varepsilon}(\omega) - \sin^2\vartheta}}$
	$\tilde{r}_p(\omega,\vartheta) = \sqrt{R_p(\omega,\vartheta)}\, e^{i\varphi_p(\omega,\vartheta)}$	$= \frac{\tilde{\varepsilon}(\omega)\cos\vartheta - \sqrt{\tilde{\varepsilon}(\omega) - \sin^2\vartheta}}{\tilde{\varepsilon}(\omega)\cos\vartheta + \sqrt{\tilde{\varepsilon}(\omega) - \sin^2\vartheta}}$
Reflectivity(+)	$R_{s,p}(\omega,\vartheta)$	$= \lvert\tilde{r}_{s,p}(\omega,\vartheta)\rvert^2$
Absorption coefficient(+)	$\mu(\omega)$	$= \frac{4\pi k}{\lambda}$
Transmission(+)(*)	$T(\omega,\vartheta)$	$= (1-R)^2\, e^{-\mu d}$

(x) - Complex; (+) - Real; (o) - The electron energy loss function found in texbooks corresponds to $-\mathcal{L}_2(\omega,\underline{q})$ defined here; (*) - The expression for transmission reported here neglects multiple reflections inside the sample.

The real and the imaginary parts of $\tilde{\varepsilon}(\omega)$ are connected with each other by the Kramers-Kronig relations:

$$\varepsilon_1(\omega) - \varepsilon_1(\infty) = \frac{2}{\pi} P \int_0^\infty \frac{\omega' \varepsilon_2(\omega')}{\omega'^2 - \omega^2}\, d\omega' \qquad (1a)$$

$$\varepsilon_2(\omega) = -\frac{2\omega}{\pi} P \int_0^\infty \frac{\varepsilon_1(\omega') - \varepsilon_1(\infty)}{\omega'^2 - \omega^2}\, d\omega' \qquad (1b)$$

and the knowledge of either one (over the entire spectral range) allows the calculation of the other. The same holds also for the real and imaginary parts of the other complex optical constants listed in Table I. Thus, from the measurement of one of the optical constants, in principle all the others can be derived.

$\varepsilon_2(\omega)$ is related to the microscopic properties of the medium and represents the probability that a photon of frequency ω is absorbed in the medium by exciting an electron to an empty state:

$$\varepsilon_2(\omega) = \frac{4\pi^2 e^2}{m\omega^2} \sum_{v,c} \int_{BZ} \frac{2\, d\underline{k}}{(2\pi)^3} \left| \underline{e} \cdot \underline{M}_{vc}(\underline{k}) \right|^2 \delta(E_c(\underline{k}) - E_v(\underline{k}) - \hbar\omega) , \qquad (2)$$

where the integration is over the entire Brillouin zone and the sum extends over all valence and conduction bands.

$$\underline{M}_{vc}(\underline{k}) = \int_{\substack{\text{crystal} \\ \text{volume}}} \psi_c^*(\underline{k}, \underline{r})\, \underline{p}\, \psi_v(\underline{k}, \underline{r})\, d\underline{r} \qquad (3)$$

is the (momentum) transition matrix element between an occupied valence state $\psi_v(\underline{k}, \underline{r})$ and an empty conduction state $\psi_c(\underline{k}, \underline{r})$. $\underline{e}$ is the unitary polarization vector of the radiation.

It is straightforward to realize that $\varepsilon_2(\omega)$ depends not only on the photon frequency, but also on the state of the medium: $\varepsilon_2 = \varepsilon_2(\omega, T, F, \ldots)$, where T represents the temperature, and F an external applied field (electric, magnetic, stress,...). Modulation spectroscopy consists of changing periodically one of those parameters and in measuring directly the variation ΔI of the optical response I of the medium, where I is either the reflectivity R or the transmission T of the medium. Since the Kramers-Kronig relations are valid also for the variation of the optical constants, usually, from the knowledge of $\Delta I/I$, it is possible to derive the variation, $\Delta\tilde{\varepsilon}$, of the dielectric function. In the limit of very small modulating amplitudes, the derivative of $\tilde{\varepsilon}$ with respect to the modulating parameter is measured directly.

Several modulation techniques, according to the parameter that one wants to change, have been developed in the quartz optic region[2,3], and most of them can be applied in the far ultraviolet as well. A sensitivity better than 10^{-4} can be easily achieved. In Table II we summarize the various modulation techniques and the materials that, to our knowledge, have been studied with synchrotron radiation modulation spectroscopy.

TABLE II

Materials studied with the different modulation techniques using synchrotron radiation. The last two methods are not proper modulation experiments, since in their case no parameter of the sample is changed, and thus they are not reviewed in this paper.

	Insulators	Metals	Semiconductors
Thermo-modulation	alkali halides	Nobel metals Transition metals Alloys	Si
Electric field modulation			III-V, Si
Magnetic field modulation		Gd, Ni	
Stress modulation			
Composition modulation		Alloys Adsorbates on metal surfaces	
Wavelength modulation	alkali halides		
Energy or wavelength derivative	yes	yes	yes

A few comments are necessary. Although synchrotron radiation from electron-synchrotrons has been used since 1966 for solid state spectroscopy[14], the discontinuous operating method of these machines resulted in very unstable sources that prevented the development of modulation spectroscopy beyond the LiF cutoff. Only storage rings, where the electrons orbit at a constant energy for several hours inside the vacuum chamber, provide a sufficiently stable source of vacuum ultraviolet radiation to make modulation spectroscopy feasable. The necessity of keeping the radiation path in a vacuum enviroment does not allow some modulation techniques that are applied succesfully below 6 eV, such as electrolyte electroreflectance, or hydrostatic pressure modulation. At very high energies, far above the plasma frequency of materials, the reflectivity drops to very small values, less than 1%. In such a case, ΔI may become of the order of, or smaller than the noise. Aspnes et al.[15] have shown that, by working at an angle of incidence near the critical angle for total external reflection (if $n < 1$), the best conditions for signal-to-noise ratio are obtained and high resolution modulation spectra can be measured. Another way to overcome this difficulty is to work in transmission on self supported thin films, following a technique developed by Rosei et al.[16]. This method has the advantage that, at high energies, since $n \approx 1$, $-\Delta T/T$ is proportional directly to $\Delta\varepsilon_2$.

Piacentini et al.[17] used a digital lock-in system at very low modulation frequencies, ~ 0.1 Hz, schematically shown in Fig. 1. The photomultiplier was operated in the analog mode and the signal

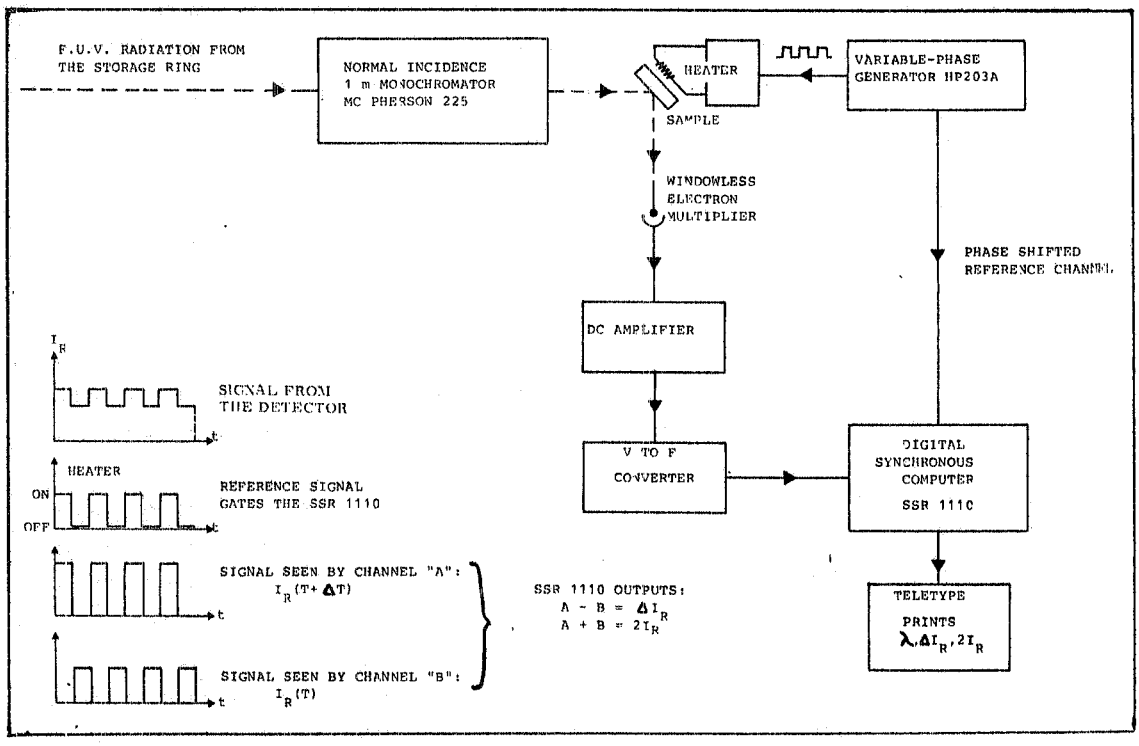

FIG. 1 - Diagram showing the low-frequency digital lock-in detection system used by Piacentini et al. (ref. 17) for thermoreflectance measurements.

amplitude was voltage-to-frequency converted and then fed into two gated counters. The gate, taken from the modulating field signal and properly phase-shifted, inhibited either counter according to the condition of field "on" or "off". After a pre-fixed number of modulating cycles, the ratio between the difference and the sum of the two counters gave the signal $2x\,\Delta I/I$. This technique, which substituted for a conventional analog lock-in, can be applied easily to the photon counting detection method.

3. - INSULATORS

3.1. - LiF

LiF is the material with the widest energy gap and is commonly used as a window between discharge vacuum ultraviolet sources and the experimental equipment. Only with the advent of synchrotron radiation could its optical properties (reflectivity and-or absorption) be measured reliably with high resolution through all the valence[10,18] as well as the Li^+1s core excitation regions, up to about 200 eV[19,20]. Previously, the use of conventional sources[21,22], as well as electron energy loss experiments[23,24,25], allowed only a rough and controversial knowledge of the electronic transitions in LiF.

From the theoretical point of view, LiF has the simplest electronic configuration of all the alkali halides. For this reason, it has been the subject of several theoretical investigations, performed mainly for the purpose of testing different approaches to the Hartree-Fock method for calculating the electron energy bands of insulators. Thus, several energy band schemes are available for LiF[26-32], but their agreement with each other and with experiment is not very good. As a matter of fact, the Hartree-Fock calculations - performed for the system in its ground state - yield energy differences between bands that are too large compared with experiment. By including correlation corrections, that account for the effects due to the electronic relaxation, polarization and electron-hole interaction in the excited crystal, the Hartree-Fock conduction and valence bands shift almost rigidly towards each other[27,30,32]. In this way the calculated energy of the fundamental gap is in good agreement with the experimental one, but the same does not occur for higher energy valence band thresholds. These corrections are not the same for the various core levels and are very difficult to calculate[29,30]. Any consequent interpretation of the core spectra could not be considered conclusive due to the nature of the approximations that were used. Finally, the broad, experimental ε_2 peak at 21.7 eV[21] was missing in the spectrum of ε_2 calculated by Mickish et al.[30] and was interpreted using a multiple-excitation model[30,33].

In the last few years photoemission, electron energy loss measurements at different values of the transferred momentum, and thermoreflectance measurements have given new insight on the above problems. By means of photoemission, in conjuction with optical spectra, the excitation threshold for the Li^+1s state was determined accurately[20,34]. The electron energy loss experiments helped to identify unequivocably some dipole-forbidden transitions, that become allowed for increasing values of the transferred momentum[35]. Thermoreflectance experiments allowed the discrimination between one-electron and multiple-electron excitations, the resolution of new structures, and led to the appearence of new problems[17,36,37].

The first prominent absorption structure in LiF is a rather sharp peak at 12.6 eV (see Fig. 2), currently interpreted as the first line of an exciton series converging to the fundamental gap $\Gamma_{15} \rightarrow \Gamma_1$[10,18,21]. The absorption line shape was reproduced by Piacentini[38], who used the Wannier model for excitons, modified to allow central cell corrections for both the energy and the oscillator strength of

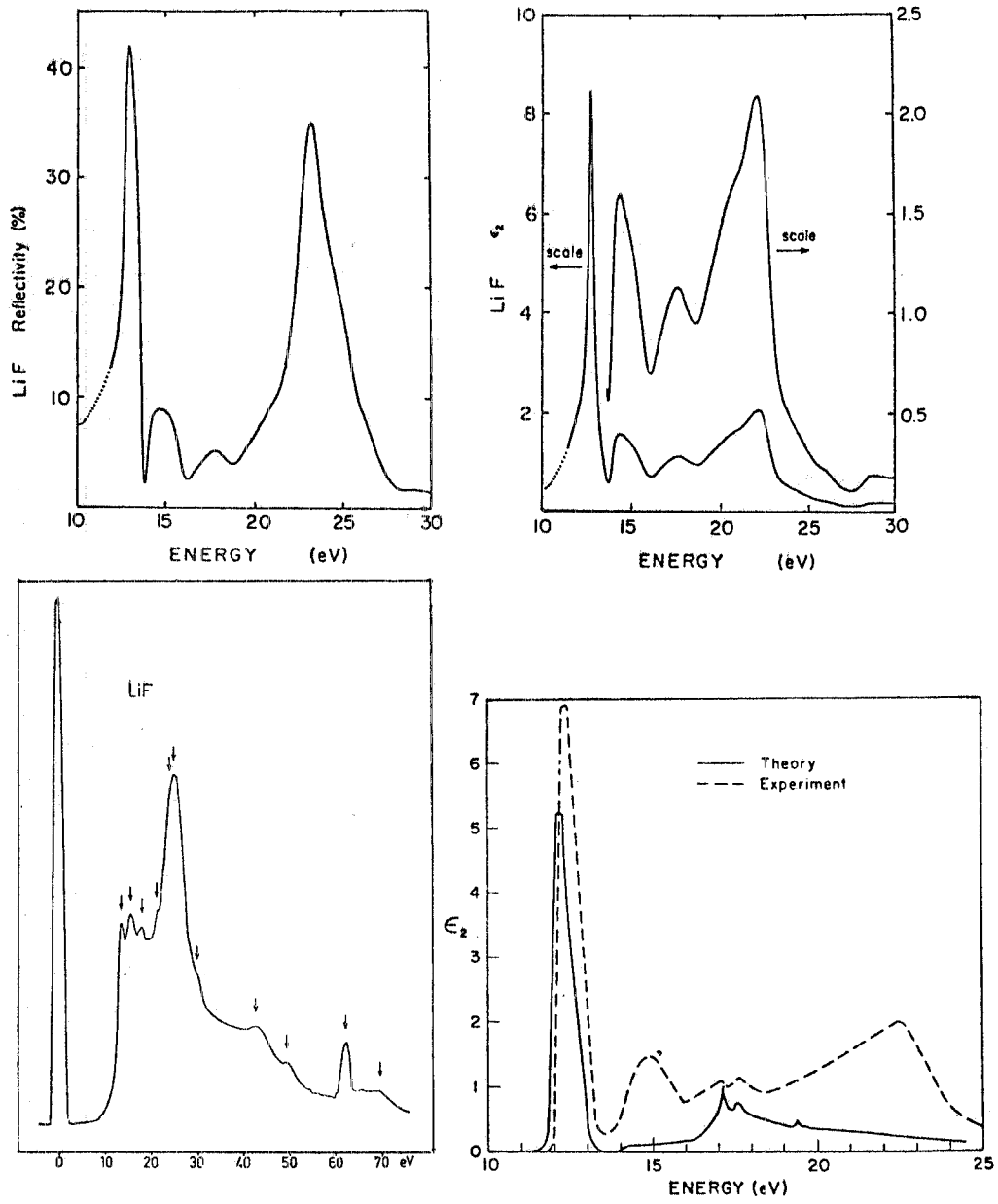

FIG. 2 - The optical spectra of LiF in the region of the valence band excitations (~10 -30 eV). a) Near normal incidence reflectivity at 100 K (after ref. 10). b) ε_2 spectrum derived by Kramers Kronig transforming the reflectivity of Fig. 2a (after ref. 10). c) Electron energy loss $\mathscr{L}_2$ spectrum for 20 KeV incident electrons (after ref. 25). d) Calculated ε_2 spectrum of LiF, compared with the experimental one obtained by G. Stephan (thesis, unpublished) (after ref. 30).

the localized n=1 exciton state. He found that the 12.6 eV peak corresponds to the n=1 state with a binding energy of 1.5 $\pm$ 0.2 eV. The higher excited states, converging to the fundamental gap, and the continuum generate the following weak, broad ε_2 structure peaking at about 15 eV. The band gap was located at 14.2 $\pm$ 0.2 eV and the exciton effective Rydberg was found of 1.0 eV.

Mickish et al.[30], instead, used the localized formalism for the exciton series. They found that the exciton wavefunction is formed mostly from states associated with a strong feature in the conduction band density of states, arising near the Brillouin zone boundary (L states), about 3 eV above the conduction band minimum. Only the n=1 line lies in the forbidden gap with an apparent binding energy of 1.8 eV, because of the strong electron-hole interaction. All the other states lie above the fundamental threshold and converge to the L point density of states structure at 17 eV. In such a way, the experimental broad structure at 15 eV, lying in a region where the calculated[30] spectrum of ε_2 is flat, was explained.

The thermoreflectance spectrum by Piacentini et al.[17,36] around the fundamental gap, as well as the thermo-modulated optical constants $\Delta\varepsilon_1$, $\Delta\varepsilon_2$ and $\Delta\mathscr{L}_2$ that have been derived from $\Delta R/R$, could be fit very well using the same equations as those used by Piacentini[38] to describe the absorption spectrum, with the same parameters for the exciton series, as shown in Fig. 3. The main contribution to the thermomodulation spectra was found to arise from a small shift to higher energies of the band gap for decreasing temperatures, in agreement with the measurements at different temperatures of Watanabe et al.[18] and of Rao et al.[10]. The variation of the line width with temperature gave only a very small contribution to the total line shape. The consistency of the fit of different experiments with the same parameters supports the modified Wannier model proposed by Piacentini[38] for the LiF fundamental excitons. This model has been confirmed recently by Zunger and Freeman[39], who obtained the excitation energies of LiF as differences between separately calculated ground and excited state configurations of a locally excited atom, viewed as a point defect placed at the center of a large unit cell. They found that the exciton series would converge to the botton of the conduction band. Similar conclusions where reached also by Fields et al.[35] from the analysis of the dispersion of the fundamental exciton as a function of the transferred momentum obtained with electron energy loss experiments.

Besides supporting the correct interpretation of the LiF fundamental exciton region, the thermoreflectance measurements gave a new contribution. In fact, Piacentini et al.[17], from the exciton-phonon interaction theory of Toyozawa[40] in the formulation proposed by Sumi[41], found that the exciton self-energy in the phonon field could be a significant fraction, as large as 30%, of the exciton binding energy.

The assignment of the next (and last) prominent valence band structure at 21.7 eV in the ε_2 spectrum of LiF to a particular transition or to a joint density of states peak is very hard, since in this region energy band calculations differ from each other. Modulation spectroscopy seems to be of little help for this purpose. But it has been very succesfull in clearing up a different interpretation based on multiple-electron excitations, and to clarify the interpretation of the electron energy loss spectra.

According to Miyakawa[42] and to Devreese et al.[33], the ε_2 structure at 21.7 eV, as well as the electron energy loss peak at 25 eV, are due to the simultaneous creation of two excitons. In particular, the theory by Devreese et al.[33], based on the electronic polaron model, predicts resonant states with a peak energy, a line shape and an oscillator strength that are in fairly good agreement with the experimental absorption and electron energy loss spectra, not only of LiF, but also of several other alkali halides. The ε_2 spectrum of LiF, calculated by Mickish et al.[30] in the one-electron approximation, is structureless between 20 and 25 eV, in support of this interpretation, as shown in Fig. 2d.

The thermomodulation spectrum of $\tilde{\varepsilon}$ showed a strong feature at 22.2 eV, corresponding to the ε_2

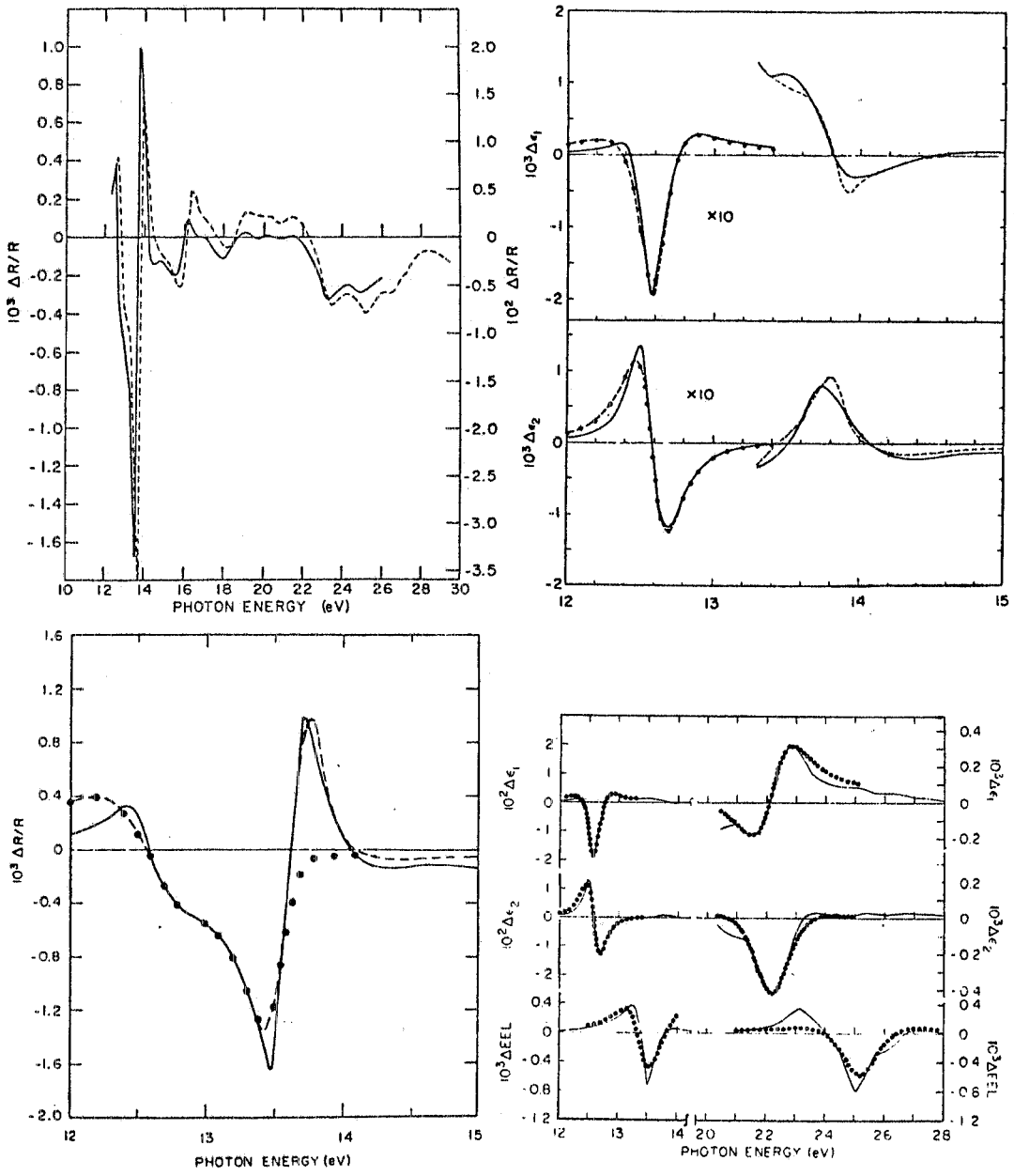

FIG. 3 - Thermomodulation spectra of LiF in the region of the valence band excitations (after ref. 17). a) Thermoreflectance spectrum. Solid line: single crystal, 1.6 Hz, $\Delta T \approx 0.4$ K (left scale). Broken line: thin evaporated film, 0.1 Hz, $\Delta T \approx 10$ K (right scale). b) $\Delta\varepsilon_1$ and $\Delta\varepsilon_2$ spectra in the fundamental exciton region. Solid line: derived by Kramers Kronig tranforms of $\Delta R/R$. Broken line: model calculation considering a modified Wannier exciton series and the continuum. Dotted line: contribution from the n=1 exciton state only. c) Fit of the $\Delta R/R$ spectrum in the fundamental exciton region calculated from the curves of Fig. 3b. Note that the structured $\Delta R/R$ line shape around 13 eV is reproduced by a single absorption peak. d) $\Delta\varepsilon_1$, $\Delta\varepsilon_2$ and $\Delta\mathcal{L}_2$ of LiF in the fundamental exciton region and around the 22 eV structure. Solid line: experimental, obtained by Kramers Kronig transforms of the $\Delta R/R$ spectrum of Fig. 3a. Dotted lines: calculated spectra (after ref. 36).

peak at 21.7 eV[17,36]. Unlike the fundamental exciton at 12.6 eV, its lineshape could be fit by considering only a modulation of the line width without any shift of the peak energy (see Fig. 3). As long as no detailed calculation on the temperature dependence of the double excitation is performed, one should expect a shift of the energy of the resonance of the same order as that of the fundamental exciton, but this was not the experimental result.

The longitudinal counterpart of the ε_2 structure at 22.2 eV occurs at 25 eV in the thermomodulation electron energy loss spectrum, as indicated in the fit shown in Fig. 3d. This structure overlaps a second feature at 24.5 eV that has not a transverse counterpart. This second feature has the characteristic line shape of a peak shifting to higher energies with decreasing temperature. Piacentini et al.[36] assigned the 24.5 eV structure to the modulation of the valence-band plasmon due to a change of the electron density. This mechanism gives also a positive background to the $\Delta\varepsilon_1$ function, that is actually observed[17,36]. This degeneracy of the longitudinal one-electron structure with the plasmon peak clearly shown by the thermomodulation spectra, accounts for and settles the controversy between the interpretations of the electron energy loss experiments[23,24,25], but it opens a new question on the co-existence of the two mechanisms. Such a degeneracy seems to be a feature common to several other alkali halides, as has been found by measuring their thermoreflectivities[36]. In their cases the interband transitions contribute with a multiplet structure degenerate with the plasmon feature.

The interpretation of the Li^+ 1s excitations between 50 and 75 eV, shown in Fig. 4, has been another subject of controversy. At the beginning the most prominent peaks in this region were attributed to

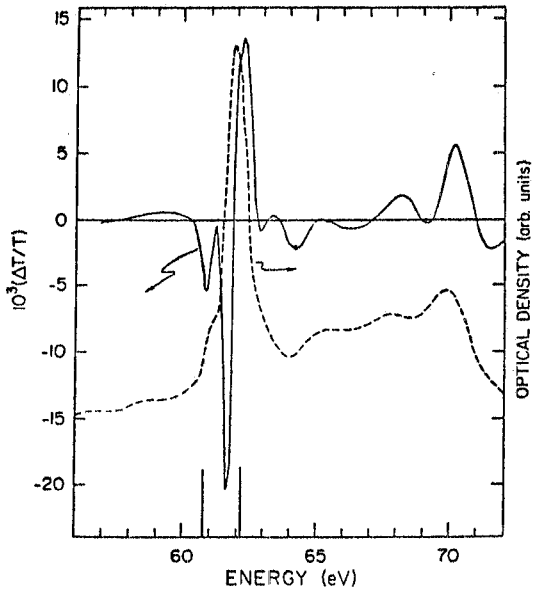

FIG. 4 - Room temperature absorption (broken line) and thermotransmission (solid line) spectra of a 230 A thick film of LiF evaporated on a 630 A thick Al film in the Li^+ 1s core exciton region (after ref. 37). The two vertical lines on the bottom correspond to the Li^+ free ion transitions $1s^2$-1s2s ^1S_o and $1s^2$-1s2p ^1P_o (after ref. 46).

exciton formation, in analogy with the fundamental absorption spectrum[43,44]. In particular, the strong peak at 61.9 eV, present in all the Li halides at almost the same energy, was assigned to the Li^+ atomic-like transition 1s – 2p. Later, a good correspondance between the experimental structures and the calculated density of states of the conduction bands was found not only in LiF but also in the other Li halides and the absorption spectrum was interpreted only in terms of one-electron transitions[19,28,29,45]. The calculated absorption threshold, associated with the bottom of the conduction band of Li^+ s-like symmetry, was found around 54 eV[28,29]. The calculated density of states was small and the oscillator strength was weak up to a first, strong p-like peak at about 63 eV, that was associated with the absorption peak at 61.9 eV[28,29,45]. Accurate absorption measurements performed by

Sonntag[45] showed weak features starting at 54 eV, in support to such an assignment.

By adding the fundamental optical gap to the Li^+ 1s binding energy relative to the top of the valence bands, as measured by photoemission, Gudat et al.[20] determined experimentally the onset of the core to conduction band transitions at 63.8 eV, in the deep absorption minimum following the most prominent peak at 61.9 eV. This procedure is represented in Fig. 5. All the structures below threshold consequently

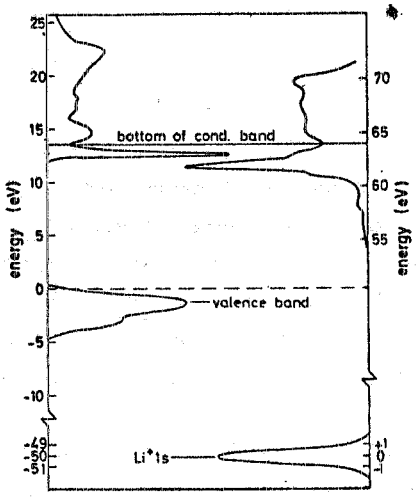

FIG. 5 - Determination of the threshold for core-state to conduction band transitions in the case of the Li^+ 1s level in LiF. Left side: valence band spectrum, as measured by XPS; the top of the valence band is used as reference energy. From the fundamental absorption spectrum, the energy of the bottom of the conduction band is determined. XPS yields also the binding energy of the Li^+ 1s state (right side); the right energy scale corresponds to the Li^+ 1s absorption spectrum, correctly aligned. The strucures lying below the bottom of the conduction bands are defined as "excitonic". (after ref. 20).

were excitonic. The 54 eV weak threshold observed by Sonntag[45] was assigned to the dipole forbidden Li^+1s - 2s transition, with a strong electron-hole interaction, and the strong 61.9 eV peak with the Li^+1s - 2p transition. Similar conclusions were reached by Pantelides and Brown[34]. In electron energy loss experiments, when the transferred momentum $\underline{q}$ is large, the "optical" dipole selection rules are relaxed and "forbidden" transitions become allowed. Fields et al.[35] found a growing structure for increasing q around 35 eV, in correspondence of the forbidden F^- 2s threshold. Instead, they did not find any structure between 50 and 60 eV, where the forbidden exciton should occur. But the weak shoulder at 61 eV, on the low energy side of the main peak at 61.9 eV, showed the proper behavior of a forbidden transition and thus it was identified as the Li^+1s $\rightarrow$ 2s atomic transition. It is worth noting that the energies of the Li^+ free ion 1s - 2s and 1s - 2p transitions[46] are close to the 61-62 eV features in LiF.

Olson and Lynch[37] gave new insight to this quite ambiguous situation performing thermotransmission experiments on LiF between 50 and 72 eV at several temperatures between 20 and 300 K. The 300 K spectrum is shown in Fig. 4. The strongest structure corresponded to the 61.9 eV exciton peak. The thermotransmission line shape was accounted for by a shift of the exciton to higher energies upon cooling, with a small contribution from the modulation of the line width. The core exciton temperature coefficient $\partial E_p / \partial T$ is almost the same as that of the fundamental exciton. On the low energy side of the exciton feature, a weaker structure is well resolved. Its line shape suggests an increase of the oscillator strength of the associated transition with increasing temperature. Olson and Lynch[37], in agreement with Fields et al.[35], assigned the 61 eV structure to the Li^+1s - 2s transition. The atomic dipole-forbidden transition becomes allowed in the solid because of the coupling with odd-parity phonons. This effect increases with temperature and so does the oscillator strength. In support of the above assignment, also the thermotransmission experiment did not give any structure below the exciton peaks, where the transmission measurements by Sonntag[45] showed weak features. Superimposed on the main feature of the allowed exciton, Olson and Lynch[37] resolved a very weak, negative peak, similar to the forbidden exciton, that was interpreted as the n=2 line of the 1s - 2s exciton series. Applying the Wannier model to the exciton series, the interband gap was calculated to be 62.5 eV, in good agreement with that

determined by Gudat et al.[20] and by Pantelides and Brown[34]. Much weaker structures are present in the thermotransmission spectra at higher energies, of difficult assignment. In particular, at 70 eV a feature, similar to that at 22 eV already discussed, was associated by Olson and Lynch[37] to interband transitions, probably to the L_3 conduction final states, in agreement with the energy band calculation by Zunger and Freeman[39]. Also for the structure at 70 eV, the electron-polaron model proposed by Devreese et al.[33] does not seem to be responsible for the observed feature.

3.2. - Other Alkali Halides

Thermoreflectance measurements have been performed on KCl and the Rb halides approximately between 10 and 30 eV by Piacentini[36,47]. All these compounds have a core threshold associated with the K^+ 3p or Rb^+ 4p states in the 17-20 eV region[48,52]. Up to about 15 eV the ε_2 spectra originate from the excitation of the valence electrons and show a strong peak, similar to the one at 22 eV already discussed for LiF. The temperature modulation of this region allowed Piacentini et al.[36] to generalize the LiF result, that in the electron energy loss spectra the plasmon is almost degenerate with several structures due to interband transitions.

In the Rb halides five well separated peaks occur between 15 and 19 eV[50-52]. Their energies do not change much upon changing the halogen ion. Their interpretation as atomic-like transitions of the type $4p^6 - 4p^5 5s$ and $4p^6 - 4p^5 4d$ localized on the Rb^+ ion is almost straightforward, since the free ion also shows the same features at approximately the same energies[46]. A similar situation is encountered in KCl[49,50] between 17 and 22 eV and its discussion follows the same scheme. By using the ligand field theory, including Coulomb and spin-orbit interactions, Satoko and Sugano[53] calculated the energies and the oscillator strengths of the Rb^+ transitions $4p^6 \rightarrow 4p^5 5s$ and $4p^6 \rightarrow 4p^5 4d$ modified and split by the cubic field. The Rb^+ ion has been treated as a deep impurity. The five strongest lines of the nine possible transitions fitted the five absorption structures observed at 77 K by Watanabe et al.[50]. However, the theory predicts at least a sixth strong line (for istance the line labelled III in Fig. 6a), not observed

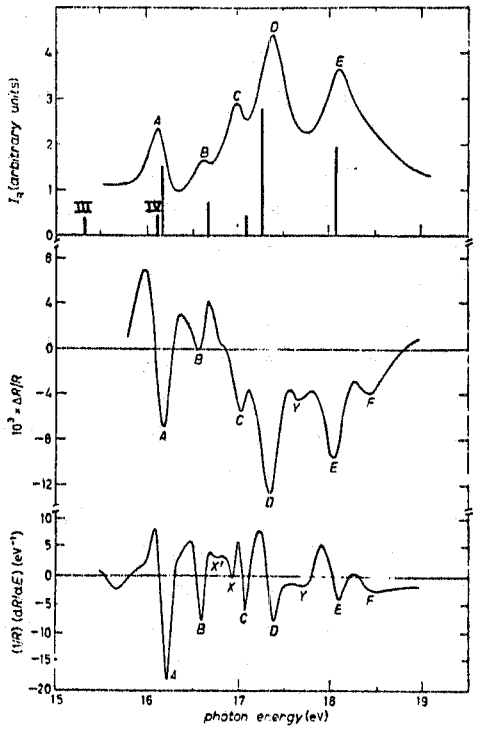

FIG. 6 - Thermoreflectance spectrum of RbBr in the Rb^+ 4p core exciton region at 200 K (middle curve) (after ref. 47). The spectrum of the radiation reflected by the sample (i.e. not corrected for the intensity of the incident radiation) is shown in the upper curve. For comparison, the wavelength modulation spectrum at 8 K measured by Zierau and Skibowski (ref. 52) is shown in the lowest curve. The vertical lines in the upper curve correspond to the transitions predicted by Satoko and Sugno (ref. 53). The heights of the lines are proportional to the calculated transition intensities.

experimentally, and it does not predict the correct temperature dependence of the exciton lines[53]. Zierau and Skibowski[52] performed wavelengh-modulated experiments at 8 K on the Rb halides, and observed some new features lying between the exciton peaks, labelled x', x, and y in Fig. 6c, that did not correspond to any of the other lines predicted by the ligand field model. The new structures were interpreted either as the onset of the continuum transitions, or as possible excited states of the excitons, or as both[52,54]. The higher sensitivity offered by the thermoreflectance technique allowed Piacentini[47] to resolve at 200 K some of the new structures found by Zierau and Skibowski[52] at 8 K. Nevertheless the missing lines were not found (cfr. Fig. 6). A tentative separation of the $\Delta\varepsilon_2$ spectrum of RbBr into the single lines[47], suggested that the lowest and the highest energy exciton lines, that are well separated from the others, follow the temperature dependence that can be inferred from the absorption spectra measured at different temperatures, i.e. a main contribution from the thermal shift of the energy of the peak and a smaller contribution from the variation of the width. Instead, for the other lines, the line shape corresponds either to a modulation of the line width or to a modulation of the exciton oscillator strenght. Piacentini[47] suggested that exciton-phonon interaction in this case tend to scatter the exitons between each other and to mix the various spectroscopic terms of the ligand field theory. In such a case, different energies and oscillator strenghts can be expected from the ligand field model.

By analogy with the LiF thermomodulation line shape around the fundamental threshold, the ionization continuum threshold was also determined for KCl and the Rb halides[47] and indicated by the arrows in Fig. 7, that refers to the thermoreflectance spectrum of KCl[55]. The threshold energy of 21.8

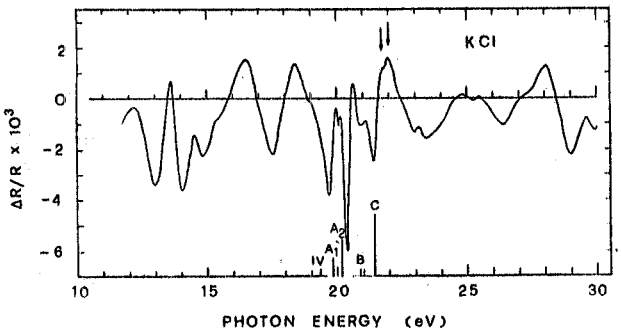

FIG. 7 - Thermoreflectance spectrum of a single crystal of KCl between 10 and 30 eV (after ref. 55). The arrows indicate the thresholds of the K^+ $3p_{5/2}$-$3p_{1/2}$ ionization continuum as determined from the thermoflectance spectrum. The vertical lines correspond to the transitions predicted by Satoko (ref. 56).

eV for the $3p_{3/2}$-conduction band transition in KCl determined in this way is in good agreement with that determined by Pantelides[57], who added the fundamental gap to the K^+ 3p binding energy as measured in photoemission. In addition, the thermoreflectance spectra clearly display the spin orbit splitting of 0.9 eV for the Rb^+ 4p states and of 0.3 eV for the K^+ 3p states, in agreement with the free ion values[46]. Finally, it must be noted that the temperature coefficient of the core excitons need not be the same as that of the fundamental gap. Instead, the temperature coefficient of the core threshold for the metal ion has opposite sign with respect to that of the fundamental gap, because of the different contribution of the Madelung potential to the energy of the valence bands with respect to the alkali core state[47].

4. - METALS

The vacuum ultraviolet absorption or reflectivity spectra of most metals[1,58,59] show broad structures, associated with either density of states features involving a large volume of the Brillouin

zone, or with the effects due to the atomic-like transition matrix element. Only at the absorption thresholds of core transitions and at very low temperatures sharp structures occur, expecially in the case of light metals. The type of modulation that can be applied most readily to metals is thermomodulation and, from the above considerations, it is not expected to give significant new contributions. Indeed, such has been the case for molybdenum[60] up to about 35 eV. Instead, all the other metals investigated[5,6,61,62,63] have shown very sharp and strong features, the interpretation of which in many cases has posed new questions, rather than answering old ones.

In spite of the smooth reflectivity, the thermoreflectance spectrum of gold revealed several new sharp features between 10 and 30 eV,[5,6] as shown in Fig. 8. Olson et al.[6] assigned these structures to

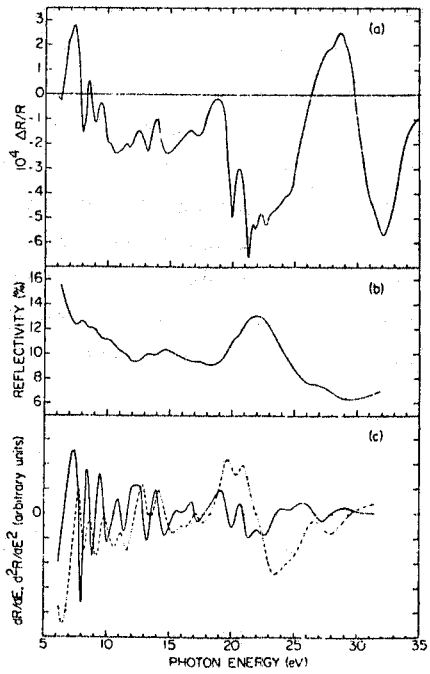

FIG. 8 - Thermoreflectance (curve a) and reflectivity (curve b) of Au at 200 K, 30° p-polarization. Curves c show the first derivative dR/dE (dashed line) and second derivative d^2R/dE^2 (full line) calculated from the reflectivity shown in Fig. 8b (after refs. 5 and 6).

critical point transitions mostly connecting the Au d bands with high-lying conduction states. The assignment was based on the energy band calculation by Connolly and Johnson,[64] but an empirical shift of some tenths of eV was applied to some of the calculated final states in order to bring into agreement the theoretical and experimental transition energies. By comparing the thermoreflectance spectrum with first and second energy derivatives of the reflectivity, Olson et al.[6] found thermal broadening to be the main source of the measured signals. The broad features between 28 and 35 eV were assigned to the temperature modulation of the two plasmon peaks observed in the electron energy loss spectra of Au at 25.8 and 32.6 eV[65].

A strong interest developed later for the region between 18 and 25 eV, where the reflectivity, as well as ε_2, shows only a broad peak, some 6 eV wide. Such a peak can be reproduced with an atomic calculation of the photoabsorption cross section of the Au 5d states[66] even with a simplified free-electron final state model[67]. This result seems to support the widespread believe that , far away from the Fermi surface, the joint density of states becomes smooth and almost structureless, converging to the free electron situation. The work by Piacentini et al.[5,6] has shown clearly that critical point transitions contribute significantly to the optical spectra even at high energies. In addition, for the first time, energy band calculations were subjected to a test far from the Fermi energy. In fact, the three strong structures at 19.9, 21.2 and 22.6 eV in the thermoreflectance spectrum of Fig. 8 were assigned by Olson et al.[6] to M_o critical point transitions beginning in the spin-orbit and crystal-field split d states

at Γ and terminating at an f-like Γ_7^- conduction state. The discrepancy of about 1.3 eV between the theoretical and the experimental position of the Γ_7^- level with respect to the Fermi energy, E_F, was of minor concern and implicitly was attributed to the inaccuracy of the theory in calculating energies so far (about 16 eV) from E_F. Instead, the d to f-like state transitions account well for the strength of the critical point transitions as well as of the broad ε_2 peak at 21 eV.

By means of constant initial state photoelectron spectroscopy, Hermanson et al.[68] found a peak at 15-16 eV above E_F in the conduction band density of states, almost at the predicted energy, invalidating the assumption of raising the final state Γ_7^- by 1.3 eV. Piacentini[47] reanalyzed the thermoreflectance spectra, obtaining by Kramers Kronig transforms the spectra of $\Delta\varepsilon_1$ and $\Delta\varepsilon_2$. He showed that only the first two structures at 19.9 and 21.2 eV dominate the $\Delta\varepsilon_2$ spectrum in the 18-25 eV region, and that the corresponding transitions occur at points of the Brillouin zone other than Γ. According to the new band structure calculation by Christensen[69], large regions of the Brillouin zone contribute to the total density of states in this energy range, probably with several, almost degenerate critical point transitions. Recently, Olson et al.[61] were able to resolve several new structures between 18 and 25 eV by means of thermotransmission measurements on unsupported Au films at 52 K, as shown in the upper curve of Fig. 9. In an attempt to assign them, they used a band-fitting procedure to the bands by Christensen[69] and

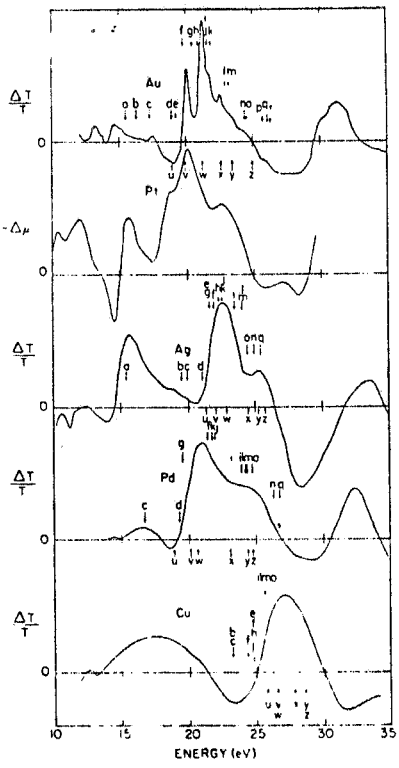

FIG. 9 - Thermotransmission spectra ($\Delta T/T = -d\Delta\mu$) for Au, Ag, Pd and Cu, and for $-\Delta\mu$ for Pt. The latter was obtained by a Kramers Kronig analysis of the thermoreflectance spectrum. The ambient temperatures are 52K for Au and about 200K for the other metals. $\Delta T/T$ is in arbitrary units and the magnitudes of two spectra cannot be compared (after ref. 61).

found over 40 critical point transitions along the symmetry lines Λ and Σ and the points Γ and L in this energy region. The identification became almost impossible. The strength of the thermotransmission structures was attributed to the degeneracy of several transitions. This interpretation did not require a shift of the final states, as it was suggested originally by Piacentini et al.[5,6]. However, recent photoemission measurements indicate that experimentally determined bands lie at higher energies than the calculated ones, the discrepancy increasing as the bands lie further from the Fermi surface[70].

Olson et al.[61] measured also the thermotransmission of unsupported films of Ag, Pd and Cu, and the thermoreflectance of Pt at about 200 K, that are shown in Fig. 9. All these metals show strong

structures, which actually are multiplets, that correspond to the Au "d-to-f" transitions between 18 and 25 eV. General trends of these transitions have been determined, that support the previous interpretation for Au, and the analyses was based on available band structure calculations as well as on photoemission data. An interesting point is about the very narrow width (less than 0.1 eV) of the structures, which is in contradiction with the measurements of 1 to 2 eV performed by Knapp et al.[71] in going from 10 to 20 eV above E_F along the Δ_1 free electron-like band of Cu. This difference, even if not yet thoroughly understood, was attributed to a possible selection rule in the decay via electron-electron scattering for f electrons.

The importance of the localized f-like character of the final states for the transitions at 19.9 and 21.2 eV suggested by Olson et al.[6] is now fully recognized. Further support was given by the reflectivity and composition-modulated reflectivity measurements performed between 18 and 35 eV by Beaglehole et al. on Au-Cu alloys[72,73,74]. The gold spectrum was found to be rather insensitive to alloying with Cu, and this was taken as evidence for localized 5f final states in the case of gold.

With the composition modulation technique, Beaglehole et al.[72] measured also the optical properties of surface films, i.e. of Cu covered with a layer of Pb or Au (25 Å and 2.5 Å thick respectively), prepared in situ, using clean Cu as reference. In both cases the bulk properties of the covering metal could explain the surface layer spectra, but some discrepancies, probably due to the interaction with the Cu substrate, have been observed.

The composition modulation technique has been used also by Cunningham et al.[75,76] to study the spectra of adsorbates on metals and oxide surfaces. They could achieve a sensitivity as low as 0.02 monolayer coverage of rare gases on substrate surfaces. For high coverages the differential spectra resembled those of the bulk spectra of the adsorbate species. Instead, for low coverages, two different behaviours were found. In some cases either the ground or the excited state switched to a new configuration and the spectra changed dramatically. Otherwise, only the local chemistry influenced the spectra. (see Fig. 10).

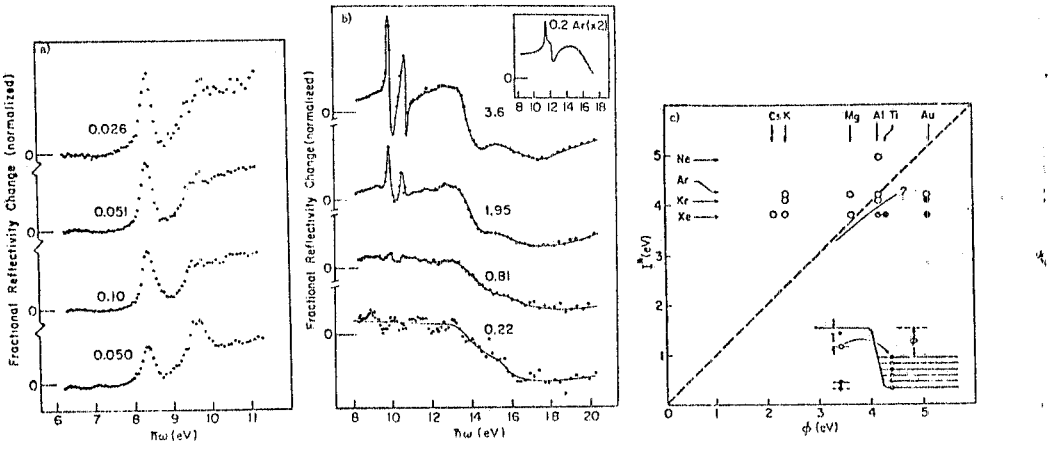

FIG. 10 - a) Fractional reflectivity changes observed for Xe on MgO substrates with p-polarized light (coverages indicated in monolayers). The data are normalized to show the effect per adsorbed atom. The lowest curve is for 130 A of MgO on Au and the remainder are for 220 A of MgO on Au. The sensisivity is photon limited beyond 9 eV with the filter, grating, and source used. (after ref. 75). b) Fractional reflectivity changes in p-polarization for Kr on Au at the coverages indicated (data normalized as in a). Analogous data for Ar on Au are shown in the inset, twice enlarged. (after ref. 75). c) Cases of persistent excitation are marked by open circles and ionic cases by full circles. The role of the excited state ionization potential I^* and the work function Φ are clearly displayed. (after ref. 76).

Olson and Lynch measured the thermotransmission of the Al $L_{2,3}$[62] and Ni $M_{2,3}$[63] absorption spectra.

The one-electron density of states just above E_F is obscured at the absorption edges of both metals by atomic effects in the case of Ni[59,77], and by many body effects in the case of Al[59,78]. Thus, mechanisms other than a thermal shift or a broadening of the structures associated with critical point or to Fermi surface transitions must underlie the strong thermomodulation signals.

Considerable controversy exists on whether many body interactions affect the K and L absorption and emission thresholds of the light metals Li, Na, Mg, and Al. This subject has been reviewed and reanalyzed in detail very recently by Citrin et al.[78] and we shall refer to their paper for a complete list of references. From their analysis, these authors concluded that many body effects, described properly by the Mahan-Nozières-De Dominicis theory[79,80], give significant contributions to the x-ray edges of the light metals. Olson and Lynch[62] have shown by means of a line shape fitting of the thermotransmission measurement, that the broadening of the Fermi function is the dominant mechanism for the temperature dependence of the edge. But the region near the spike could not be fit well and several mechanisms were discussed as responsible for the discrepancy. Some could be ruled out easily - for instance, a temperature shift of the edge may give the correct contribution to the line shape, but it requires a shift three orders of magnitude higher than the one that might actually occur - but for the others the question is left open.

The $M_{2,3}$ absorption threshold of metallic Ni[77,81,82] is interpreted in terms of the atomic-like transition $3p^6 3d^9 \rightarrow 3p^5 3d^{10}$, which is degenerate and interferes with the continuum of the $3p^6 3d^9 \rightarrow 3p^6 3d^8 \varepsilon f$ transitions[77,83,84]. The lineshape has the well known Fano resonance structure[85]:

$$\mu(E) = \mu_o \frac{(q+\varepsilon)^2}{(1+\varepsilon)^2} \quad . \tag{4}$$

Here μ_o is the absorption coefficient for the unperturbed continuum, $\varepsilon = (E-E_\Phi - F)(\Gamma/2)^{-1}$ is the reduced energy (Γ is the line width parameter, E_Φ is the energy of the discrete level and F is its self-energy due to the interaction) and q is the interference parameter between the discrete line and the continuum. The experimental value of q determined from the fit was a factor 2-2.5 times smaller than the theoretical one. This discrepancy is not yet understood and is attributed to possible solid state effects. Composition modulation experiments were performed by Gudat and Kunz[86] on a Cu-Ni 1:1 alloy versus a sandwich film containing both constituents on top of each other. Within the experimental accuracy no difference could be detected, showing that in the alloy both atoms behave independently from each other, in support to the atomic picture. Instead, in the case of Ni-Al alloys, a remarkable difference could be observed around both the Al $L_{2,3}$ and the Ni $M_{2,3}$ edges[86,87,88]. The comparison between the Ni thresholds measured in the metal and in the vapor[77,89] is of little help, since the two spectra are sufficiently similar to favor the atomic mechanism, but differences must be attributed to solid state effects. Thus, the role of solid state effects on the $M_{2,3}$ absorption threshold of Ni is not yet understood.

The thermotransmission measurement by Olson and Lynch[61], displayed in Fig. 11, showed that the $M_{2,3}$ edge of Ni depends strongly on temperature, which is indeed a solid state effect. The experimental spectrum could be fit by the temperature derivative of the Fano line shape eq. (3), using the parameters known from static measurements. The dependence from temperature of the structure enters through the reduced energy ε and the interference parameter q. Both terms depend from a common microscopic parameter, the square of the interaction matrix element between the discrete line and the continuum. In addition to it, the strongest temperature dependence of ε was found to originate from the resonance

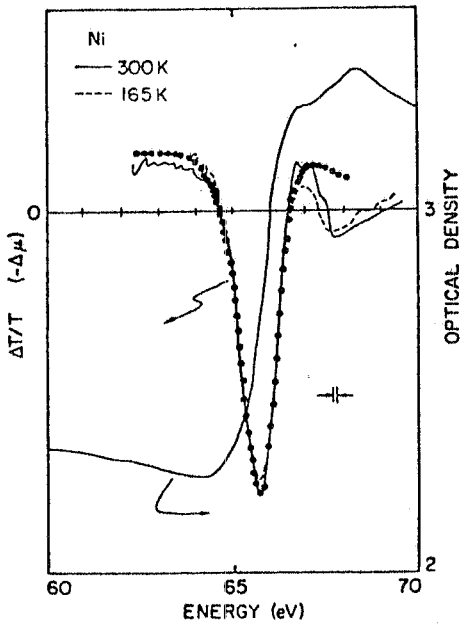

FIG. 11 - Optical density and thermotransmission at 300K for Ni in the region of the $M_{2,3}$ edges. The dots are a fit to the temperature derivative of the Fano line shape, representing the M_3 edge only, for q=0.9, Γ=2.0 eV. The plot is -(0.6 $d\mu/dq$ + 1.4 $d\mu/d\varepsilon$) in arbitrary units. The coefficients 0.6 and 1.4 represent the temperature derivatives of q and ε, respectively. (Note that for Γ=2.0 eV, one unit in ε corresponds to 1.0 eV). (after ref.63).

energy E_Φ - F. It is not clear why these atomic parameters should be so sensitive to temperature.

Magneto-optical measurements have been performed by Erskine on Ni[90] and Gd[90,91]. In the case of Gd[90,91] the purpose of the research has been to pin-point the absorption threshold of the localized 4f electrons. The 4f states can be excited to either 5d final states or to g states. The former have a smaller, but more concentrated oscillator strength and generate a broad bump in the conductivity of Gd between 5 and 11 eV[92]. The oscillator strength of the latter is spread and delayed over a wide energy range and at threshold it is very weak. XPS measurements[93] yield a binding energy for the 4f states of about 8 eV, which sets the excitation threshold at energies too high with respect to the conductivity feature. On the other hand, an analysis of the sum rules performed on the conductivity spectrum sets the threshold at 6.1 eV[91,92]. 4f electrons are strongly spin polarized, and should give strong magneto-optical signals[94]. The magneto-optical spectra were obtained by measuring, at several angles of incidence, the reflectivity of p-polarized radiation from a sample magnetized in the surface plane and perpendicular to the plane of incidence[90,91]. A change of the reflected intensity occurs upon magnetization reversal because of the different absorption of left and right circularly polarized light. This different absorption is represented by $\sigma^{(2)}_{xy}$, the imaginary part of the off-diagonal term of the conductivity tensor[95]. The intensity and sign of the magneto optical structures are directly related to the degree and to the sign of the spin-polarization of the electrons in their initial state. Below 6 eV $\sigma^{(2)}_{xy}$ shows weak structures associated with the excitation of the p bands to empty d-like states[94]. The ratio between peak intensities is in agreement with theoretical estimates. Unlike the p electrons, 4f electrons are essentially 100% polarized and much stronger structures of the same sign as the p structure are expected, even if the oscillator strength is weak. Two strong peaks occur at 6.1 and 8 eV respectively, showing even very fine structures, as shown in Fig. 12. The first one is in agreement with the previous determination of the threshold[88]. The superimposed fine structure is attributed to the final state configuration $4f^6 5d$, that gives a multiplet spread over about 1 eV. The threshold determined by the magneto optical method is about 2 eV lower than the binding energy of the 4f states as measured by XPS[93]. This difference, as well as the presence of a second threshold at 8 eV, has been explained in terms of different screening configurations around the 4f hole.

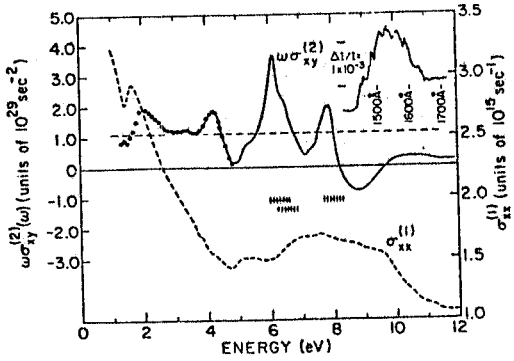

FIG. 12 - Magneto-optical spectrum of Gd. $\sigma_{xy}^{(2)}$ is the absorptive component of the off-diagonal elements of the conductivity tensor $\overleftrightarrow{\sigma}$. $\sigma_{xx}^{(1)}$ is the absorptive component of the diagonal elements of $\overleftrightarrow{\sigma}$. Dotted line: previous data obtained using ellipsometric methods. Solid line: data obtained using synchrotron radiation and the transverse configuration as described in the text. Inset: structure at the 8-eV peak. Broken horizontal line: intraband component of $\sigma_{xy}^{(2)}$ (after ref. 91).

5. - SEMICONDUCTORS

More than for the other groups of materials, modulation spectroscopy has been applied to semiconductors for a systematic study of the electronic properties of III-V compounds. Electroreflectance measurements have been performed by Aspnes et al. on GaAs, GaP and GaSb from 6 to 30 eV with the Schottky barrier technique under different experimental conditions[96-102]. The GaAs spectrum is shown in Fig. 13. A detailed review of these experiments has appeared recently[7,103], so that we shall limit our discussion to only the most significant results obtained from the electromodulation spectra of the Ga 3d core states.

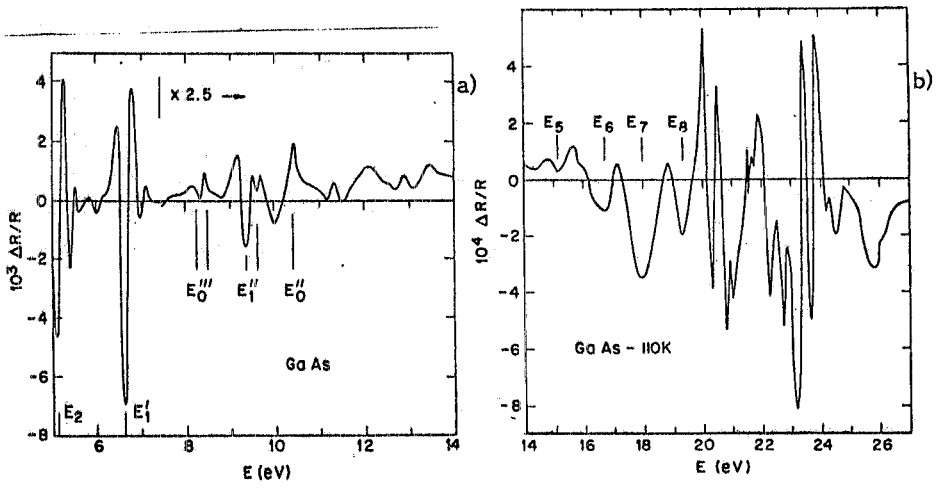

FIG. 13 - a) Electroreflectance of GaAs 5-14 eV. b) Electroreflectance of GaAs 14-27 eV. (after refs. 7, 97).

Since the width of the Ga 3d bands is approximately 0.1 meV[104], within the one-electron approximation electroreflectance structures can be related directly to the conduction band critical points. The assignment of the electroreflectance structures to the lowest conduction band minima has been rather straightforward in the case of GaP[96,97], but for GaAs there has been some difficulty. Only after high resolution experiments at 60° and a detailed calculation of the transition matrix elements,

Aspnes et al.[99] could assign the first three structures at 20.02, 20.32 and 20.76 eV to the Γ_6^c, L_6^c and X_6^c minima respectively. In fact, from the calculation of the transition matrix elements and the use of the density of states effective masses, the electroreflectance structure associated with X_6^c should be the strongest, the L_6^c about half as large and the Γ_6^c quite small. Such a trend is followed by the first three structures with the above order, as shown in Fig. 14. This result was very important, since it reversed the

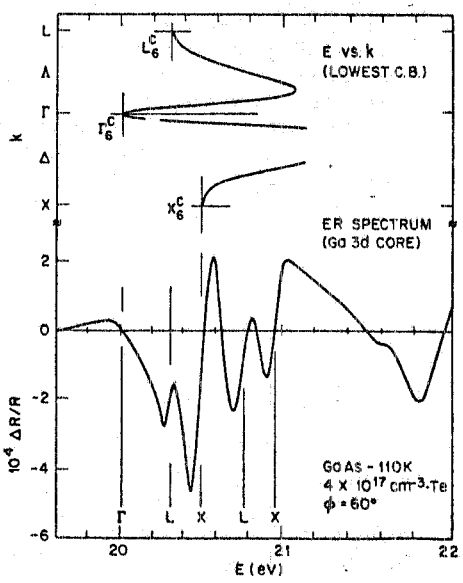

FIG. 14 - Fine structure in the electroreflectance Ga 3d core-level threshold of GaAs, with assignments to conduction band minima. (after ref. 7).

ordering previously accepted for several years[105] and it has been supported by recent calculations of the band structure using a non-local pseudopotential scheme[106,107]. In addition, many recent experiments could find a rather simple explanation, as discussed thoroughly by Aspnes[102].

From the electroreflectance spectra, Aspnes et al.[100] obtained $\Delta\varepsilon_1$ in the region of the core transitions. The $\Delta\varepsilon_1$ spectrum was separated into two components originating from the $d_{5/2}$ and $d_{3/2}$ levels respectively, with the latter structures shifted by the spin-orbit splitting of 0.45 ± 0.02 eV of the Ga 3d level, and with an intensity reduced by a factor of 2/3, corresponding to the statistical ratio between the two levels. Finally, the spectrum of $\Delta\varepsilon_1$ from the $d_{5/2}$ level only was fit using the Franz-Keldysh formulas of Blossey[108] for an exciton associated with a three dimensional M_0 singularity. The parameters obtained from the fit were the lifetime broadening of 160 meV and the exciton effective Rydberg R_{ex}=160 meV. The fit was very good, as shown in Fig. 15 and the second zero crossing at 20.48

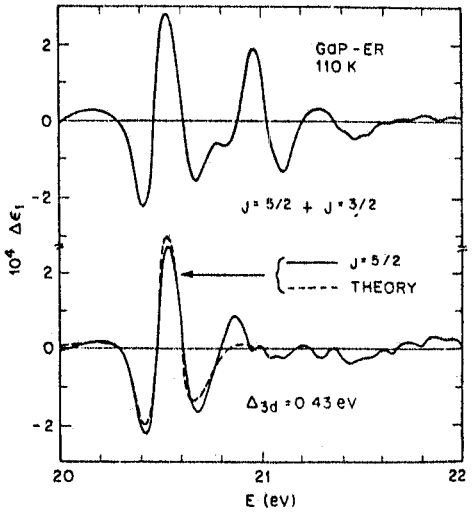

FIG. 15 - Top: $\Delta\varepsilon_1(E)$ for GaP for the Ga 3d-lower sp^3 conduction band transitions at 110 K. Bottom: Comparison of the j= 5/2 component with lifetime-broadened Coulomb-enhanced Franz-Keldysh theory (after ref. 100).

eV was associated with the energy $E_g - R_{ex}$. In this way the exciton effective Rydberg was obtained directly, with a single measurement. The determination of excitonic effects, suggested by Gudat et al.[20] for LiF and already discussed, requires the addition of the core level binding energy (referred to the top of the valence bands) to the optical fundamental gap, in order to obtain the threshold energy E_T for a free core-hole electron pair. Any structure in the photoabsorption spectrum associated with that particular core state lying below E_T is assigned to core excitons. This method, applied to the III-V compounds using the XPS data of Ley et al.[109] and compared with the electroreflectance X_6^c feature, yielded exciton binding energies of 170 ± 150 meV for GaP and 90 ± 250 meV for GaAs[7,110] and GaSb[7,101,110]. The large error, mainly due to the determination of the top of the valence bands in the XPS spectra, makes the excitonic effect rather dubious, even if confirmed by later determinations. The main point is the value of R_{ex} obtained, which is much larger than the value for the excitons associated with the fundamental gap, as well as than any reasonable determination from the effective mass approximation[7,111]. The value obtained by Aspnes et al.[100] from the fitting of the electromodulation $\Delta \varepsilon_1$ line shape is in perfect agreement with the previous determination and confirms it. Large excitonic effects have been observed also in the case of other seminconductors, but not yet explained[111].

Additional evidence for large values of R_{ex} has been given by Bauer et al.[112] in the case of the Si $L_{2,3}$ threshold at about 100 eV. Around threshold, the Si spectrum is completely different from the one-electron density of states[113,114]. Altarelli and Dexter[115] could fit its lineshape within the effective mass theory for excitons, obtaining an effective Rydberg of 40 meV. Instead, Bauer et al.[112] derived an exciton Rydberg of 0.6 ± 0.2 eV comparing the $L_{2,3}$ binding energy that they measured with available absorption data[113,114]. Margaritondo and Rowe[116] compared electron energy loss and XPS data measured on the same reconstructed 7 x 7 Si surface, and found R_{ex}=0.9 ± 0.4 eV. But, with such a large binding energy, one should be able to resolve the n=1 and the n=2 exciton lines[117], which is not the case. Bauer et al.[112] measured the electroreflectance at the Si $L_{2,3}$ edge, but they could not detect any signal within the experimental sensitivity. This null result was interpreted as due to exciton formation with a binding energy larger than 300 meV, in agreement with the previous determinations. These large values of the binding energy imply that the excitation is strongly localized around a single atom. In support of this point, the absorption measurements by Brown et al.[117] on the $L_{2,3}$ threshold of heavily doped Si samples (up to 10^{20} donors per cm^3) did not show any change in position or line shape, suggesting that the excitation should be localized within the 20 Å screening length in those samples[112].

Thermomodulation experiments[118], as well as electroflectance measurements at different temperatures[98], have furnished valuble information on the temperature behavior of core level excitations. In the case of the Ga 3d transitions in GaP, the thermal shift of structures was attributed to the temperature dependence of the final states only[98]. Instead, the Si 2p levels seem to be strongly affected by temperature[118]. The core level shift was attributed to the change of the electrostatic potential at the 2p core as a result of a temperature induced redistribution of valence charge. The different behavior between the two materials was ascribed to the larger volume occupied by the Ga 3d levels, which feel a more averaged potential.

CONCLUSIONS

Modulation spectroscopy using synchrotron radiation as a light source in the vacuum ultraviolet and soft x-ray regions has been reviewed. Even if this type of experiments started several years ago, not much work has been done. The reason may stem on the difficulty of having the light source available, or

on the difficulty in interpreting the results. As a matter of fact, the optical measurements suffer by the limitation that several transitions, degenerate in energy, take place at the same photon energy and it is very difficult to separate them. Instead, angle resolved photoemission spectroscopy is much more powerful from this point of view, and thus presently it is preferred to optical measurements.

Nevertheless, the results obtained until now have shown clearly the full potentiality of modulation spectroscopy also above 10 eV, in particular in the case of core transitions. Several problems have been cleared, such as the controversy on the double-excitations versus one-electron excitations in alkali halides (cfr. Sect. 3.1. and 3.2.), or the ordering of the conduction bands of GaAs (cfr. Sect. 5.). In other cases new problems have been opened, onto which a great deal of new studies have been performed, as in the case of the Au "d-to-f" transitions. Finally, there are still some results which are not understood in detail.

Thus, we feel that modulation spectroscopy with synchrotron radiation is still a very important tool for studying the electronic properties of solids. Beyond an extensive application of the techniques already employed to a variety of samples, new experiments, for instance of crossed effects, should be developed in order to clear some open questions. The technique of composition modulation seems particularly promising, since it opens the field of surface studies also to the optical method.

ACKNOWLEDGEMENTS

The author is strongly indebt to F. Antonangeli, A. Balzarotti, F. Bassani, and D.W. Lynch for a critical reading of the manuscript.

The collaboration of L. Invidia, S. Stipcich, and of all the staff of the Documentation Service of the Laboratori Nazionali of Frascati, given at different stages of preparation of this manuscript has been higly appreciated.

REFERENCES

(1) For the most recent review on this subject, see: "Synchrotron Radiation Techniques and Applications", in "Topics in Current Physics", C. Kunz ed. (Springer, 1979), vol. 10.
(2) M. Cardona, "Modulation Spectroscopy" (Academic Press, 1967).
(3) "Semiconductors and Semimetals", R.K. Willardson and A.C. Beer eds. (Academic Press, 1972), vol. 9.
(4) E.M. Rowe, R.A. Otte, C.H. Pruett, and J.D. Steben, IEEE Trans. Nucl. Sci. NS16, n°3, p. 159 (1969).
(5) M. Piacentini, C.G. Olson,and D.W. Lynch, Proc. 4th Inter. Conf. on Vacuum Ultraviolet Radiation Physics, Hamburg 1974, E.E. Koch, R. Haensel, and C. Kunz eds. (Pergamon, 1974).
(6) C.G. Olson, M. Piacentini, and D.W. Lynch, Phys. Rev. Letters 33, 644 (1974).
(7) D.E. Aspnes, "Modulation Spectroscopy with Synchrotron Radiation" in "Advances in Solid State Physics", J. Treush ed. (Vieweg Braunschweig, 1977) vol. 17, p. 235.
(8) D.W. Lynch, J. Phys. 39, C4-125 (1978).
(9) D.W. Lynch, in ref. 1, p. 357.
(10) K.K. Rao, T.J. Moravec, J.C. Rife, and R.N. Dexter, Phys. Rev. B12, 5937 (1975).
(11) See, for istance, G. Martinez, M. Schlüter, M.L. Cohen, R. Pinchaux, P. Thiry, D. Dagneaux, and Y. Petroff, Solid State Commun. 17, 5 (1975); also D.E. Aspnes, M. Cardona, V. Saile, M. Skibowski, and G. Sprüssl, Solid State Commun. 31, 99 (1979).

(12) F. Stern, Solid State Phys. 15, 300 (1963).
(13) F. Wooten, "Optical Properties of Solids" (Academic Press, 1972).
(14) P. Jaegle and G. Missoni, Comptes Rendus 262, 71B (1966).
(15) D.E. Aspnes, C.G. Olson, and D.W. Lynch, J. Appl. Phys. 47, 602 (1976).
(16) R. Rosei, M. Meuti, C. Coluzza, and C. Quaresima, Opt. Letters 1, 217 (1977).
(17) M. Piacentini, D.W. Lynch, and C.G. Olson, Phys. Rev. B13, 5530 (1976).
(18) M. Watanabe, H. Nishida, and A. Ejiri, Proc. 4th Intern. Conf. on Vacuum Ultraviolet Radiation Physics, Hamburg 1974, E.E. Koch, R. Haensel, and C. Kunz eds. (Pergamon, 1974) p. 370.
(19) F.C. Brown, C. Gähwiller, A.B. Kunz, and N.O. Lipari, Phys. Rev. Letters 25, 927 (1970).
(20) W. Gudat, C. Kunz, and H. Peterson, Phys. Rev. Letters 32, 1370 (1974).
(21) D.M. Roessler and W.C. Walker, J. Phys. Chem. Sol. 28, 1507 (1969).
(22) A.P. Lukirskii, O.A. Ershov, T.M. Zimkina, and P. Savinov, Sov. Phys. Solid State 8, 1422 (1966).
(23) O. Sueoka, J. Phys. Soc. Jpn. 20, 2226 (1965).
(24) M. Creuzburg and H. Raether, Solid State Commun. 2, 175 (1964).
(25) C. Gout and F. Pradal, J. Phys. Chem. Sol. 29, 581 (1968).
(26) A.B. Kunz, T. Miyakawa, and S. Oyama, Phys. Stat. Sol. 34, 581 (1969).
(27) F. Perrot, Phys. Stat. Sol. (b) 52, 163 (1972).
(28) W.P. Menzel, C.C. Lin, D.F. Fouquet, E.E. Lafon, and R. Chaney, Phys. Rev. Letters 30, 1313 (1973).
(29) A.B. Kunz, D.J. Mickish, and T.C. Collins, Phys. Rev. Letters 31, 756 (1973).
(30) D.J. Mickish, A.B. Kunz, and T.C. Collins, Phys. Rev. B9, 4461 (1974).
(31) R.N. Euwema, A.A. Wepfer, G.T. Surrot, and D.L. Wilhite, Phys. Rev. B9, 5249 (1974).
(32) N.E. Brener, Phys. Rev. B11, 1600 (1975).
(33) J.T. Devreese, A.B. Kunz, and T.C. Collins, Solid State Commun. 11, 673 (1972).
(34) S.T. Pantelides and F.C. Brown, Phys. Rev. Letters 33, 298 (1974).
(35) J.R. Fields, P.C. Gibbons, and S.E. Schnatterly, Phys. Rev. Letters 38, 430 (1977).
(36) M. Piacentini, C.G. Olson, and D.W. Lynch, Phys. Rev. Letters 35, 1658 (1975).
(37) C.G. Olson and D.W. Lynch, Solid State Commun. 31, 51 (1979).
(38) M. Piacentini, Solid State Commun. 17, 679 (1975).
(39) A. Zunger and A.J. Freeman, Phys. Rev. B16, 2901 (1977).
(40) Y. Toyozawa, Progr. Theor. Phys. 20, 53 (1958).
(41) H. Sumi, J. Phys. Soc. Jpn. 82, 616 (1972).
(42) T. Miyakawa, J. Phys. Soc. Jpn. 17, 1898 (1962).
(43) R. Haensel, C. Kunz, and B. Sonntag, Phys. Rev. Letters 20, 262 (1968).
(44) A. Maiste, A.M. Saar, and M.A. Elango, Sov. Phys. Solid State 16, 1118 (1974).
(45) B.F. Sonntag, Phys. Rev. B9, 3601 (1974).
(46) C.E. Moore "Atomic Energy Levels as Derived from Analysis of Optical Spectra", U.S. National Bureau of Standards, Circular n° 467 (U.S. GPO, Washington, 1949).
(47) M. Piacentini, Nuovo Cimento 39B, 682 (1977).
(48) D. Blechschmidt, R. Haensel, E.E Koch, U. Nielsen, and M. Skibowski, Phys. Stat. Sol. (b) 44, 787 (1971).
(49) G. Sprüssel, M. Skibowski, and V. Saile, 14th Inter. Conf. Phys. Semiconductors Edimburgh 1978, ed. by B.L.H. Wilson (Inst. Phys. Bristol, Conf. Ser. 43, 1978), p. 1359.
(50) M. Watanabe, A. Ejiri, H. Yamashita, H. Sato, S. Sato, T. Shibaguchi, and H. Nishida, J. Phys. Soc. Jpn. 31, 1085 (1971).
(51) V. Saile, N. Schwentner, M. Skibowski, W. Steinmann, and W. Zierau, Phys. Letters 46A, 245 (1973).
(52) W. Zierau and M. Skibowski, J. Phys. C: Solid State Phys. 8, 1671 (1975).
(53) C. Satoko and S. Sugano, J. Phys. Soc. Jpn. 34, 701 (1973).
(54) C. Satoko and S. Sugano, Proc. 4th Intern. Conf. on Vacuum Ultraviolet Radiation Physics, Hamburg 1974, E.E. Koch, R. Haensel, C. Kunz eds. (Pergamon 1974) p. 368.
(55) M. Piacentini, unpublished.
(56) C. Satoko, Solid State Commun. 13, 1851 (1973).
(57) S.T. Pantelides, Phys. Rev. B11, 2391 (1975).
(58) F.C. Brown, Solid State Phys. 29, 1 (1975).
(59) C. Kunz, "Optical Properties of Solids - New Developments", B.O. Seraphin ed. (North Holland, 1975), p. 473.
(60) J.H. Weaver, C.G. Olson, D.W. Lynch, and M. Piacentini, Solid State Commun. 16, 163 (1975).
(61) C.G. Olson, D.W. Lynch, and R. Rosei, Phys. Rev. B22, 593 (1980).
(62) C.G. Olson and D.W. Lynch, Solid State Commun. 31, 601 (1979).
(63) C.G. Olson and D.W. Lynch, Solid State Commun. 33, 849 (1980).
(64) J.W.D. Connolly and K.H. Johnson, Massachussets Institute of Technology, Solid State and Molecular Theory Group, Report n° 72 (1970) p. 19.
(65) M. Creuzburg, Z. Phys. 196, 433 (1966).
(66) F. Combet Farnoux and Y. Heno, Comptes Rendus, 264, B138 (1967).
(67) D. Beaglehole, Proc. Phys. Soc. London, 85, 1007 (1965).
(68) J. Hermanson, J. Anderson, and G. Lapeyre, Phys. Rev. B12, 5410 (1975).
(69) N.E. Christensen, Phys. Rev. B13, 2698 (1976).

(70) R. Rosei, R. Lässer, N.V. Smith, and R.L. Bembow, Solid State Commun. 35, 979 (1980), and references therein.
(71) J.A. Knapp, F.J. Himpsel, and D.E. Eastman, Phys. Rev. B19, 4952 (1979).
(72) D. Beaglehole, M. De Crescenzi, B. Thieblemont, Nguyen Binh, M.L. Theye, and G. Vuye, Proc. 5th Intern. Conf. on Vacuum Ultraviolet Physics, Montpellier 1977, M.C. Castex, M. Pouey, N. Pouey eds. (CNRS, 1978), vol. II, p. 73.
(73) D. Beaglehole and B. Thieblemont, Nuovo Cimento B39, 477 (1977).
(74) D. Beaglehole, M. De Crescenzi, M.L. Theye, and G. Vuye, Phys. Rev. B19, 6303 (1979).
(75) J.E. Cunningham, D. Greenlow, C.P. Flynn, and J.L. Erskine, Phys. Rev. Letters 42, 328 (1979).
(76) C.P. Flynn, Proc. VI Intern. Conf. on Vacuum Ultravioler Radiation Physics, Charlottesville 1980.
(77) B. Sonntag, J. Phys. 39, C4-9 (1978).
(78) P.H. Citrin, C.H. Wertheim, and M. Schlüter, Phys. Rev. B20, 3067 (1979).
(79) G.D. Mahan, Phys. Rev. 163, 612 (1967).
(80) P. Nozières and C.T. De Dominicis, Phys. Rev. 178, 1097 (1969).
(81) B. Sonntag, R. Haensel, and C. Kunz, Solid State Commun. 7, 597 (1969).
(82) F.C. Brown, C. Gähwiller, and A.B. Kunz, Solid State Commun. 9, 487 (1971).
(83) R. Dietz, E.G. Mc Rae, Y. Yafet, and C.W. Caldwell, Phys. Rev. Letters 33, 1372 (1974).
(84) L.C. Davis and L.A. Feldkamp, Solid State Commun. 19, 413 (1976).
(85) U. Fano, Phys. Rev. 124, 1866 (1961).
(86) W. Gudat and C. Kunz, Phys. Stat. Sol. (b) 52, 433 (1972).
(87) H.J. Hagemann, W. Gudat, and C. Kunz, Solid State Commun. 15, 566 (1974).
(88) H.J. Hagemann, W. Gudat, and C. Kunz, Phys. Stat. Solidi (b) 71, 507 (1976).
(89) R. Bruhn, B. Sonntag, and H.W. Wolff, J. Phys. B12, 203 (1979).
(90) J.L. Erskine, Physica B89, 83 (1977).
(91) J.L. Erskine, Phys. Rev. Letters 37, 157 (1976).
(92) J.L. Erskine and C.P. Flynn, Phys. Rev. B14, 2197 (1976).
(93) F.R. Mc Feely, S.P. Kowalczyk, L. Ley, and D.A. Shirley, Phys. Letters 45A, 227 (1973).
(94) J.L. Erskine and E.A. Stern, Phys. Rev. B8, 1239 (1973).
(95) H.S. Bennett and E.A. Stern, Phys. Rev. A137, 448 (1965).
(96) D.E. Aspnes and C.G. Olson, Phys. Rev. Letters 33, 1605 (1974).
(97) D.E. Aspnes, C.G. Olson, and D.W. Lynch, Phys. Rev. B12, 2527 (1975).
(98) D.E. Aspnes, C.G. Olson, and D.W. Lynch, Phys. Rev. Letters 36, 1563 (1976).
(99) D.E. Aspnes, C.G. Olson, and D.W. Lynch, Phys. Rev. Letters 37, 766 (1976).
(100) D.E. Aspnes, C.G. Olson, and D.W. Lynch, Phys. Rev. B14, 2534 (1976).
(101) D.E. Aspnes, C.G. Olson, and D.W. Lynch, Phys. Rev B14, 4450 (1976).
(102) D.E. Aspnes, Phys. Rev. B14, 5331 (1976).
(103) D.E. Aspnes, Nuovo Cimento 39B, 337 (1977).
(104) J.C. Phillips, Phys. Rev. Letters 22, 285 (1969)
(105) H. Ehrenreich, Phys. Rev. 120, 1951 (1960).
(106) K.C. Pandey and J.C. Phillips, Phys. Rev. B9, 1552 (1974).
(107) J.R. Chelikowsky and M.L. Cohen, Phys. Rev. Letters 32, 674 (1974), Phys. Rev. B14, 556 (1976).
(108) D.F. Blossey, Phys. Rev. B3, 1382 (1971).
(109) L. Ley, R.A. Pollak, F.R. Mc Feely, S.P. Kowalczyk, and D.A.Shirley,Phys. Rev. B9, 600 (1974).
(110) D.E. Aspnes, C.G. Olson, and D.W. Lynch, Proc. 13th Intern. Conf. on Physics Semiconductors, F.G. Fermi ed. (Marves, Rome 1976), p. 1000.
(111) A. Quattropani, F. Bassani, G. Margaritondo, and G. Tinivella, Nuovo Cimento 51B, 409 (1977).
(112) R.S. Bauer, R.Z. Bachrach, J.C. Mc Menamin, and D.E. Aspnes, Nuovo Cimento 39B, 409 (1977).
(113) C. Gähwiller and F.C. Brown, Phys. Rev. B2, 1918 (1970).
(114) F.C. Brown and O.P. Rustgi, Phys. Rev. Letters 28, 497 (1972).
(115) M. Altarelli and D.L. Dexter, Phys. Rev. Letters 29, 110 (1972).
(116) G. Maragaritondo and J.E. Rowe, Phys. Letters 59A, 464 (1977).
(117) F.C. Brown, R.Z. Bachrach, and M. Skibowski, Phys. Rev. B15, 4781 (1977).
(118) D.E. Aspnes, R.S. Bauer, R.Z. Bachrach, and J.C. Mc Menamin, Phys. Rev. B16, 5436 (1977).